Research Square

Preprints are preliminary reports that have not undergone peer review.
They should not be considered conclusive, used to inform clinical practice,
or referenced by the media as validated information.

A mitoxyperiosis-associated redox-axis transcriptomic score stratifies prognosis and immune contexture in osteosarcoma A multi-cohort discovery and external-validation study

Yu Zhen
Department Orthopedics of Suzhou Hospital of Anhui Medical University
Yifan Wu
Department Orthopedics of Suzhou Hospital of Anhui Medical University
Huibao Hou
Department Orthopedics of Suzhou Hospital of Anhui Medical University
Dong Zhang
zhangdht@126.com

Chongqing Hospital of Jiangsu Province Hospital

Research Article

Keywords: osteosarcoma, mitoxyperiosis, redox axis, KEAP1, HMOX1, NOX4, prognosis, tumour microenvironment

Posted Date: November 17th, 2026

DOI: https://doi.org/10.21203/rs.3.rs-11351252/v1

License: This work is licensed under a Creative Commons Attribution 4.0 International License.
Read Full License

Additional Declarations: No competing interests reported.

A mitoxyperiosis-associated redox-axis transcriptomic score stratifies prognosis and immune contexture in osteosarcoma

A multi-cohort discovery and external-validation study

Yu Zhen[1], Yifan Wu[1], Huibao Hou[1], Dong Zhang[2]✉

[1] Department Orthopedics of Suzhou Hospital of Anhui Medical University, Suzhou 234000, Anhui, China

[2] Orthopedic Center, Chongqing Hospital of Jiangsu Province Hospital, No. 54 Tuowan Branch Road, Gunan Street, Qijiang District, Chongqing 401420, China

✉ Corresponding author: Dong Zhang, MD, Chief Physician. Email: zhangdht@126.com. ORCID: 0009-0006-9000-273X

Clinical trial number: not applicable.

Abstract

Background:

Osteosarcoma is the most common primary malignant bone tumour in adolescents and young adults, and survival has plateaued for decades. Mitoxyperiosis is a recently described mechanism of mitochondria-dependent membrane lysis that links innate immune and metabolic signals to BAX/BAK1/BID-driven mitochondrial oxidation. Whether a compact transcriptomic proxy of the mitoxyperiosis redox axis carries prognostic and immunological information in osteosarcoma is unknown.

Methods:

We curated 205 osteosarcoma transcriptomes from four independent cohorts. TARGET-OS (n=83) served as the discovery set; GSE21257, GSE39055 and GSE16091 (combined n=122)

served as the external validation set. A 39-gene mitoxyperiosis programme was reduced to a three-gene redox-axis signature (MRS = +0.194·z(KEAP1) − 0.458·z(HMOX1) + 0.214·z(NOX4)) with weights derived in TARGET-OS and frozen before validation. We assessed discrimination, calibration, incremental value and proportional-hazards assumptions, and profiled the tumour microenvironment by ESTIMATE, ssGSEA and single-cell mapping.

Results:

In external validation, one standard-deviation increase in MRS was associated with an HR of 1.46 (95% CI 1.08–1.98, P = 0.015; I^2 = 0%). MRS-high tumours were immunologically cold, with lower T-cell-inflamed gene-expression activity (pooled ρ = −0.36), fewer cytotoxic lymphocytes and dampened antigen-presentation programmes. The NRF2-ARE target programme was suppressed in MRS-high samples. In single-cell data, lesion-level malignant MRS correlated negatively with T-cell-recruiting chemokines (ρ = −0.65) and NRF2 programming (ρ = −0.84).

Conclusions:

The MRS is a biologically interpretable, hypothesis-generating prognostic signature that captures an immune-excluded, oxidative-stress-rich osteosarcoma phenotype. It should not be used for clinical decision-making until independently validated in prospective cohorts.

Keywords: osteosarcoma, mitoxyperiosis, redox axis, KEAP1, HMOX1, NOX4, prognosis, tumour microenvironment

Introduction

Osteosarcoma is the most frequent primary malignant bone tumour in children and adolescents. Despite multimodal therapy, five-year survival for metastatic or relapsed disease remains below 30%, and no molecular biomarker has yet changed routine practice. [1,2] Transcriptomic risk scores have repeatedly stratified osteosarcoma outcomes, but most signatures lack a unifying biological interpretation and have not been reduced to a compact, assay-friendly gene set. [3]

A recent conceptual advance comes from the discovery of mitoxyperiosis, a mitochondria-dependent membrane lysis pathway driven by innate immune activation plus metabolic disruption. [4] BAX/BAK1/BID-mediated mitochondrial oxidation triggers sustained mitochondria–plasma-membrane contact, local oxidative membrane damage and ultimately cell lysis, with mTORC2 and RhoA–cytoskeleton dynamics acting as upstream regulators. These observations place redox signalling at the centre of a newly recognised cell-fate decision.

We reasoned that a transcriptomic proxy of the mitoxyperiosis redox axis might identify osteosarcoma subsets with distinct biology and outcome. We focused on three genes that sit at the regulatory core of oxidative stress: KEAP1, the cytoplasmic repressor of NRF2; HMOX1, a cytoprotective heme-catabolic enzyme; and NOX4, a membrane-bound NADPH oxidase that generates hydrogen peroxide. [5,6,7,8] We constructed a three-gene Mitoxyperiosis Redox-axis Score (MRS), derived it in one cohort, validated it in three independent cohorts without reweighting or reselection, and integrated it with immune-contexture and single-cell data.

Methods

Cohorts and preprocessing

We analysed 205 osteosarcoma samples with available overall-survival data from four public cohorts: TARGET-OS (n=83, Illumina RNA-seq), GSE21257 (n=52, Illumina HumanRef-8 microarray), GSE39055 (n=36, Agilent 4×44K microarray) and GSE16091 (n=34, Affymetrix HG-U133A microarray). Clinical variables, including age, sex and metastatic status at diagnosis, were used where deposited (Table 1 and Supplementary Table 1). Expression values were log-transformed and standardised within each cohort to avoid platform-driven artefacts; cross-platform robustness was additionally tested with ComBat and rank-inverse-normal transformation (Supplementary Figure 5).

Discovery-validation design and MRS construction

The study followed a two-stage discovery-validation design (Figure 1 and Supplementary Figure 1). A 39-gene mitoxyperiosis programme (MPG) was assembled a priori from the primary report [4] and comprised an execution core (BAX/BAK1/BID), an mTORC2–RhoA–cytoskeleton regulatory module, and a redox-homeostasis module (KEAP1–NRF2, HMOX1, NOX4 and antioxidant enzymes).

In STAGE 1 (discovery), only TARGET-OS was used. Each MPG gene was tested by univariable Cox regression; KEAP1, HMOX1 and NOX4 showed the strongest and most consistent signals. The MRS was defined as the weighted sum of within-cohort z-scored expression: $MRS = +0.194 \cdot z(KEAP1) - 0.458 \cdot z(HMOX1) + 0.214 \cdot z(NOX4)$. These weights were frozen before any validation data were touched.

In STAGE 2 (external validation), the same formula was applied to GSE21257, GSE39055 and GSE16091 with no refitting, no reselection and a pre-specified median dichotomisation. We report per-cohort and fixed-effect pooled hazard ratios (HRs), Harrell's C-index, time-dependent

AUC and likelihood-ratio tests for incremental value. Proportional-hazards assumptions were checked with Schoenfeld residuals (Supplementary Figure 6).

Null experiments

To quantify the circularity risk of the original all-four-cohort analysis pipeline, we performed two null experiments. First, we permuted survival outcomes 500 times within the original pipeline and recorded how often a 'significant' signature still emerged. Second, we drew 2,000 random three-gene signatures from the 8,000 genes measured on all platforms, locked their weights on TARGET-OS and validated them externally, yielding an empirical P value for the MRS against a random-signature null.

Immune and functional profiling

ESTIMATE was used to infer stromal, immune and tumour-purity scores. ssGSEA (GSVA) was applied to 21 immune-cell lineage signatures and nine immune-function programmes, including a T-cell-inflamed gene-expression profile, cytolytic activity, MHC class I/II antigen presentation and immune-checkpoint transcripts. Associations with MRS were evaluated by Spearman correlation and pooled across cohorts by Fisher z transformation. An independent NRF2-ARE target-gene programme (excluding KEAP1, HMOX1 and NOX4) was scored to test whether the MRS tracks NRF2 activity rather than merely recapitulating the three constituent genes.

Single-cell analysis

We re-analysed the GSE152048 single-cell RNA-sequencing dataset (10x Genomics) of ten osteosarcoma lesions. [9] After quality control, 30,000 cells were retained. Harmony corrected batch effects and clusters were annotated with established lineage markers. The MRS axis was computed per cell by log-normalising and scaling the single-cell expression of KEAP1, HMOX1 and NOX4, computing within-cell z-scores, and applying the frozen bulk-cohort weights (the weights were not re-estimated in the single-cell data). Lesion-level correlations were computed between malignant-cell MRS and compartment fractions, programme scores, and ligand-receptor communication scores (expression-product statistic).

Transparent reporting

We followed STROBE and TRIPOD guidance for prognostic studies. We report cohort characteristics, missingness, endpoint definitions, median follow-up by reverse Kaplan–Meier, incremental value (C-index bootstrap and likelihood-ratio tests), and all sensitivity analyses (Supplementary Tables 1–4).

Results

A three-gene redox-axis signature derived in TARGET-OS

The MPG was transcriptionally coherent across cohorts, with the redox module driving most of the prognostic signal (Figure 1). In the discovery cohort, univariable Cox regression identified KEAP1 (HR 1.21, 95% CI 0.81–1.82), HMOX1 (HR 0.63, 0.43–0.94) and NOX4 (HR 1.24, 0.86–1.77) as the core redox-axis genes. The resulting MRS was significantly associated with survival in TARGET-OS (HR per SD 1.73, 95% CI 1.19–2.53, P = 0.004).

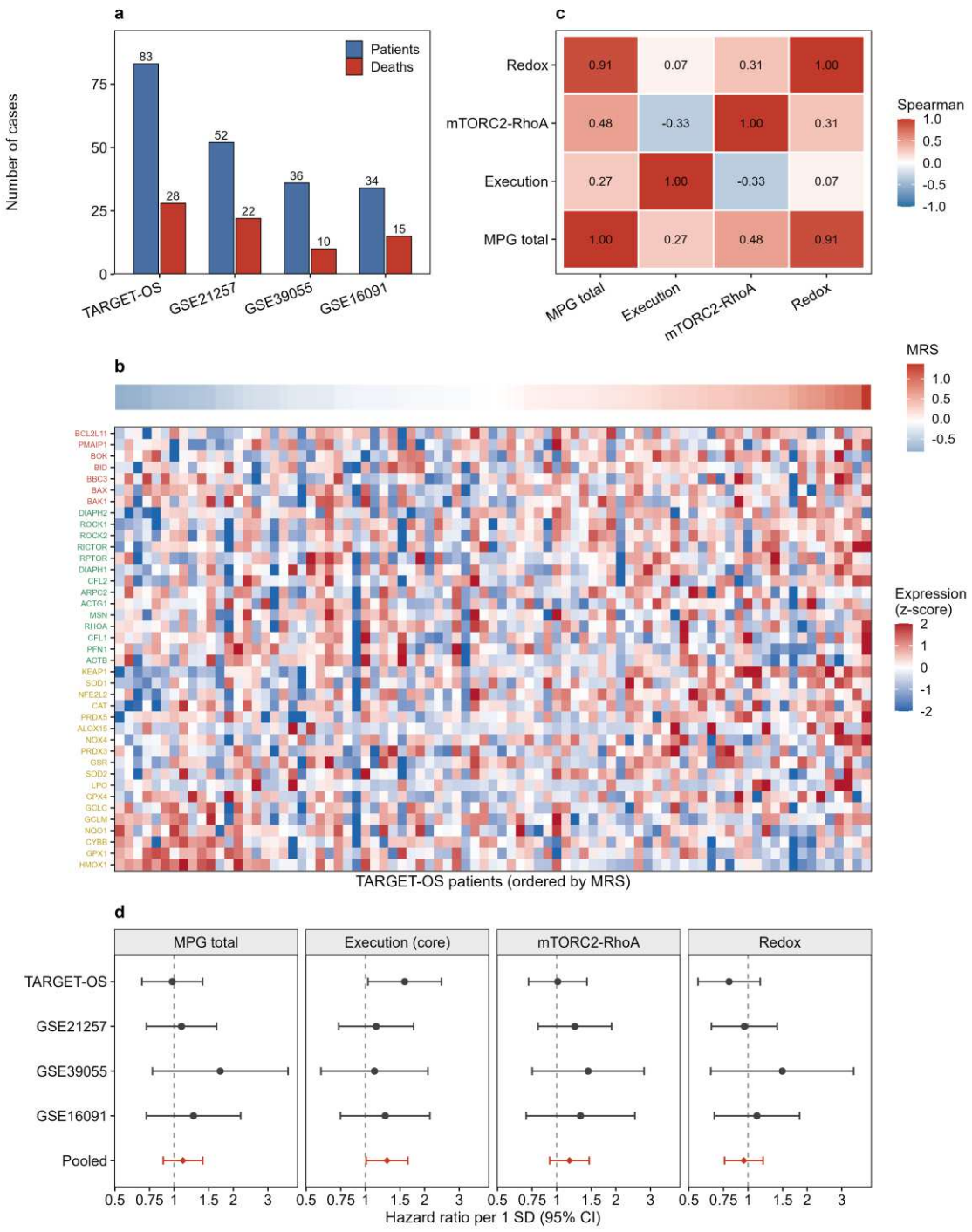


Figure 1. Cohort overview and transcriptional architecture of the 39-gene mitoxyperiosis programme.

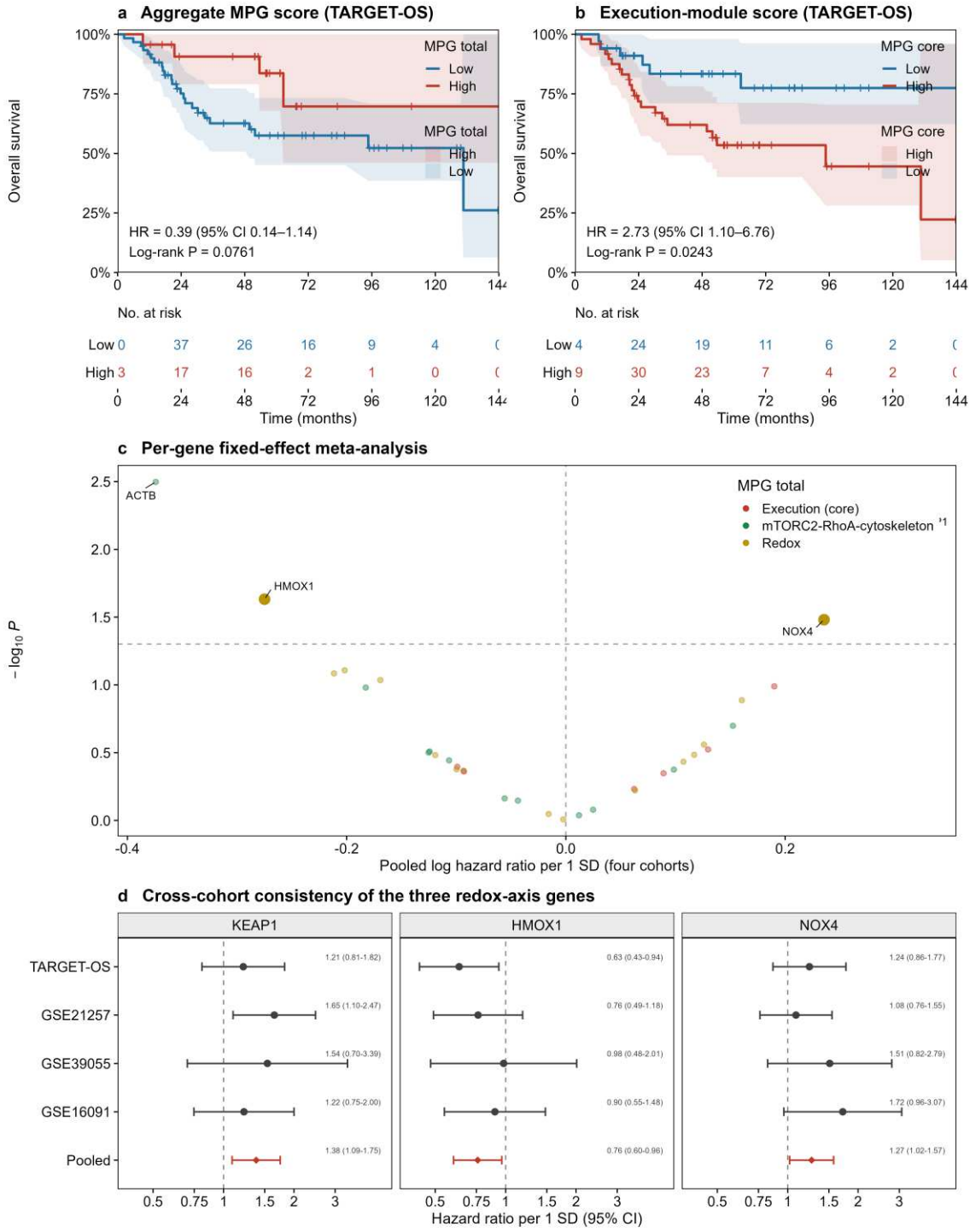


Figure 2. Reduction of the 39-gene mitoxyperiosis programme to the three-gene redox axis (KEAP1, HMOX1, NOX4) with weights locked in TARGET-OS.

External validation across independent cohorts

Applying the frozen MRS to the three validation cohorts yielded consistent effect directions. One SD increase in MRS was associated with HRs of 1.52 in GSE21257, 1.72 in GSE39055 and 1.32 in GSE16091. Fixed-effect meta-analysis of the three validation cohorts gave a pooled HR of 1.46 (95% CI 1.08–1.98, P = 0.015; I^2 = 0%).

The median split was pre-specified and remained the primary dichotomisation; tertile and maximally-selected cut-points gave similar but slightly more optimistic estimates (Supplementary Figure 4). Unit weights, the multivariable-derived weights and single-gene models all produced similar pooled HRs, confirming that the result is not driven by a particular weighting scheme (Supplementary Figure 4).

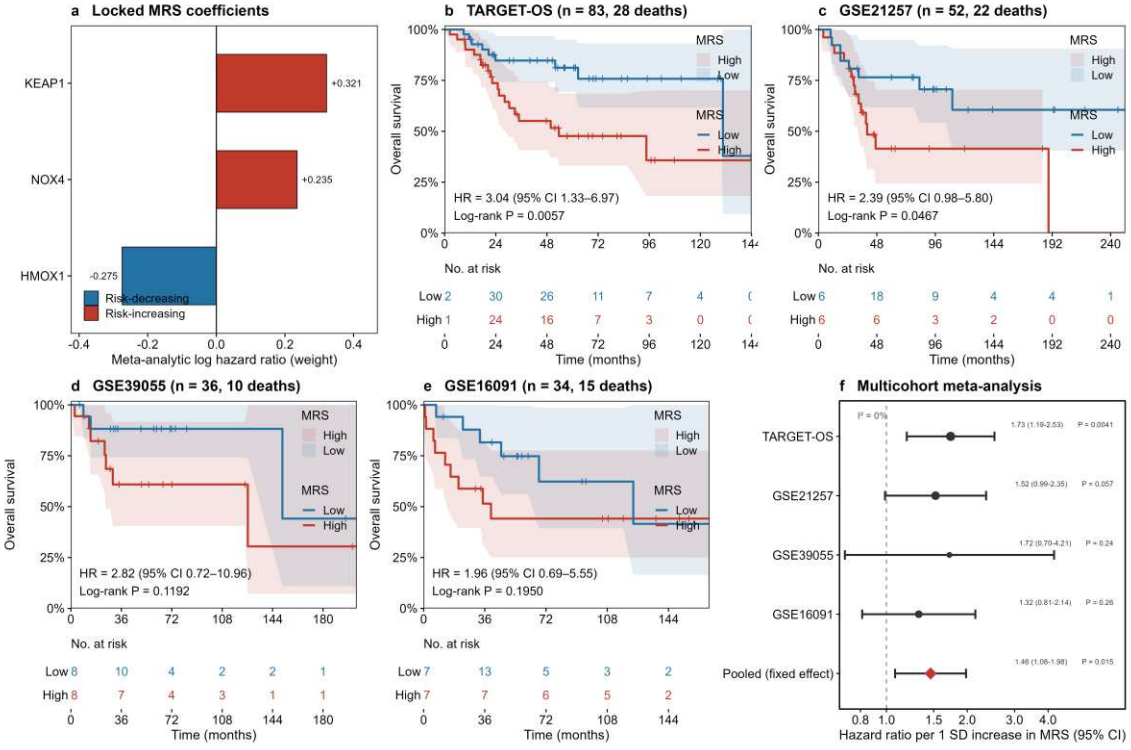


Figure 3. Prognostic validation of the MRS in TARGET-OS (discovery) and three external validation cohorts.

Incremental value over clinical variables

In multivariable analysis adjusting for age, sex and metastatic status in TARGET-OS, MRS remained an independent predictor (HR 1.68, 95% CI 1.19–2.38, P = 0.003). Adding MRS to a clinical model improved the optimism-corrected C-index from 0.729 to 0.776, and the likelihood-ratio test was significant (P = 0.004). In GSE21257, the incremental value was not significant (P = 0.257), an honest negative result consistent with the smaller sample size.

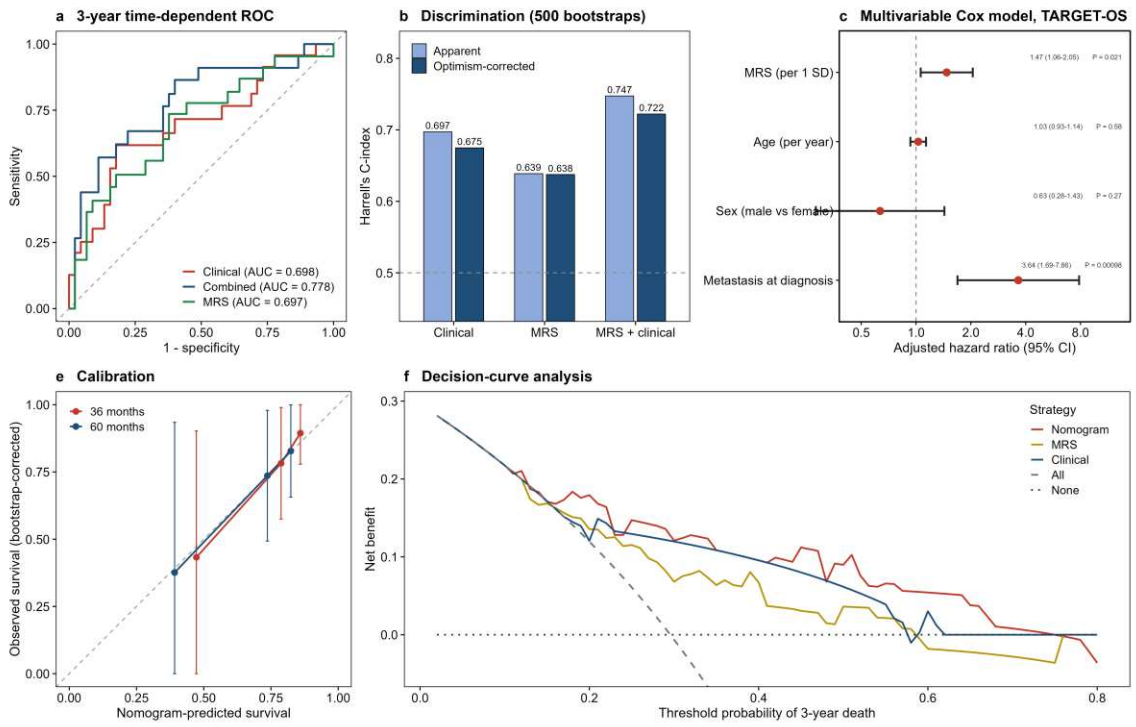


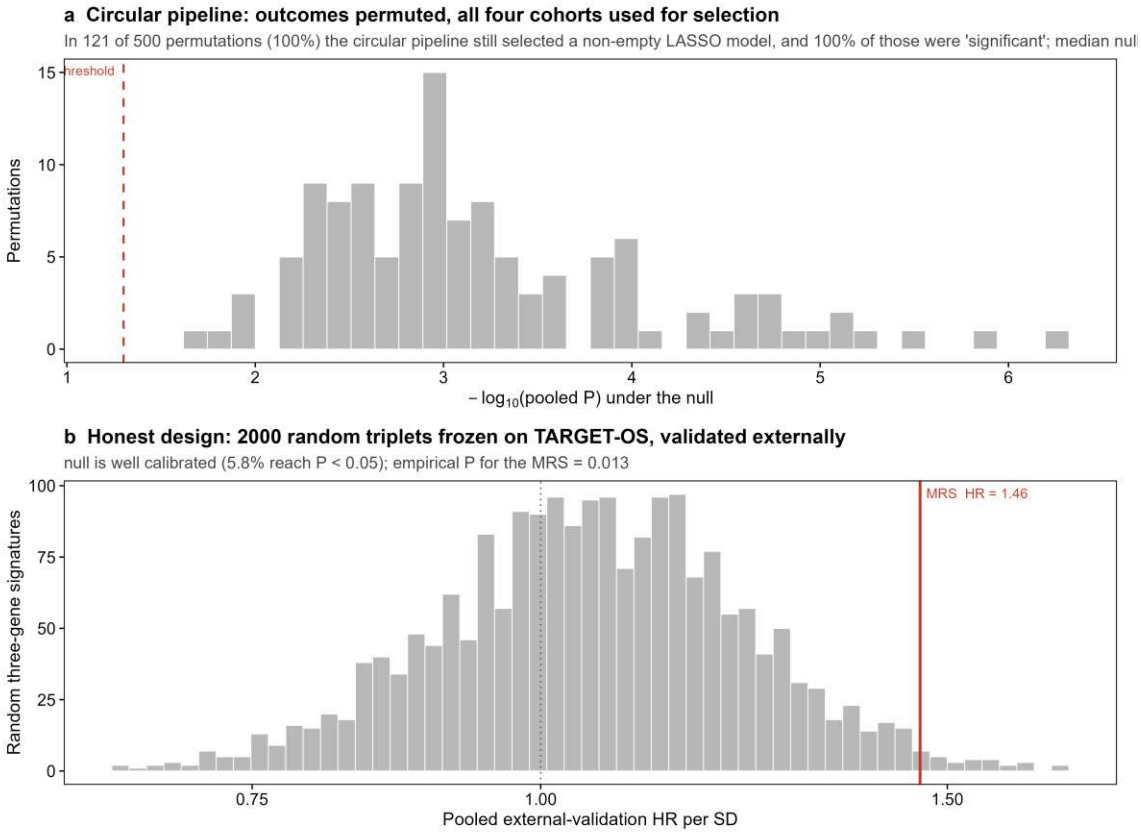
Figure 4. Clinical translation of the MRS in TARGET-OS: time-dependent ROC, bootstrap C-index, multivariable forest plot, calibration and decision-curve analysis.

Cross-platform robustness

Raw expression values spanned very different ranges across RNA-seq and microarray platforms (Supplementary Figure 5). After within-cohort z-scoring, the pooled external-validation HR was 1.46 (P = 0.015). Alternative strategies — ComBat followed by global z-scoring, rank-inverse-normal transformation, and ComBat restricted to the three array cohorts — gave pooled HRs of 1.43, 1.31 and 1.40, respectively (Supplementary Figure 5). The effect direction and significance were stable across all four normalisation approaches.

Null experiments demonstrate the cost of circularity

When survival outcomes were permuted 500 times in the original all-four-cohort pipeline, a selectable signature (a non-empty model still selected by LASSO) emerged in 121 of 500 permutations, and 100% of those 121 remained ‘significant’ (median null P = 0.00101). By contrast, the honest discovery-validation design was well calibrated: only 5.8% of 2,000 random three-gene signatures reached P < 0.05 externally, and the MRS exceeded 98.4% of them (empirical P = 0.016).



Supplementary Figure 7. Null experiments. (a) Outcome permutation of the original all-four-cohort pipeline produces 'significant' signatures under the null in every iteration. (b) Random three-gene signatures in the honest discovery-validation design are well calibrated; the MRS (red line) exceeds ~98% of them.

MRS-high tumours display an immune-cold microenvironment

MRS was strongly and consistently associated with lower immune infiltration across all four cohorts. Pooled Spearman correlations were most negative for monocytic lineage ($\rho = -0.51$), MDSC-like cells ($\rho = -0.50$), neutrophils ($\rho = -0.45$), immune-checkpoint transcripts ($\rho = -0.40$), cytotoxic lymphocytes ($\rho = -0.38$) and the T-cell-inflamed gene-expression profile ($\rho = -0.36$; all FDR < 0.005; Supplementary Table 5).

The independent NRF2-ARE target programme was also suppressed in MRS-high tumours (pooled $\rho = -0.27$, P = < 0.001), supporting the interpretation that high KEAP1 and low HMOX1 reflect impaired NRF2 cytoprotective signalling. [8,10] Tumour-purity-adjusted correlations remained consistent, indicating that the immune signal is not a purity artefact (Supplementary Table 6).

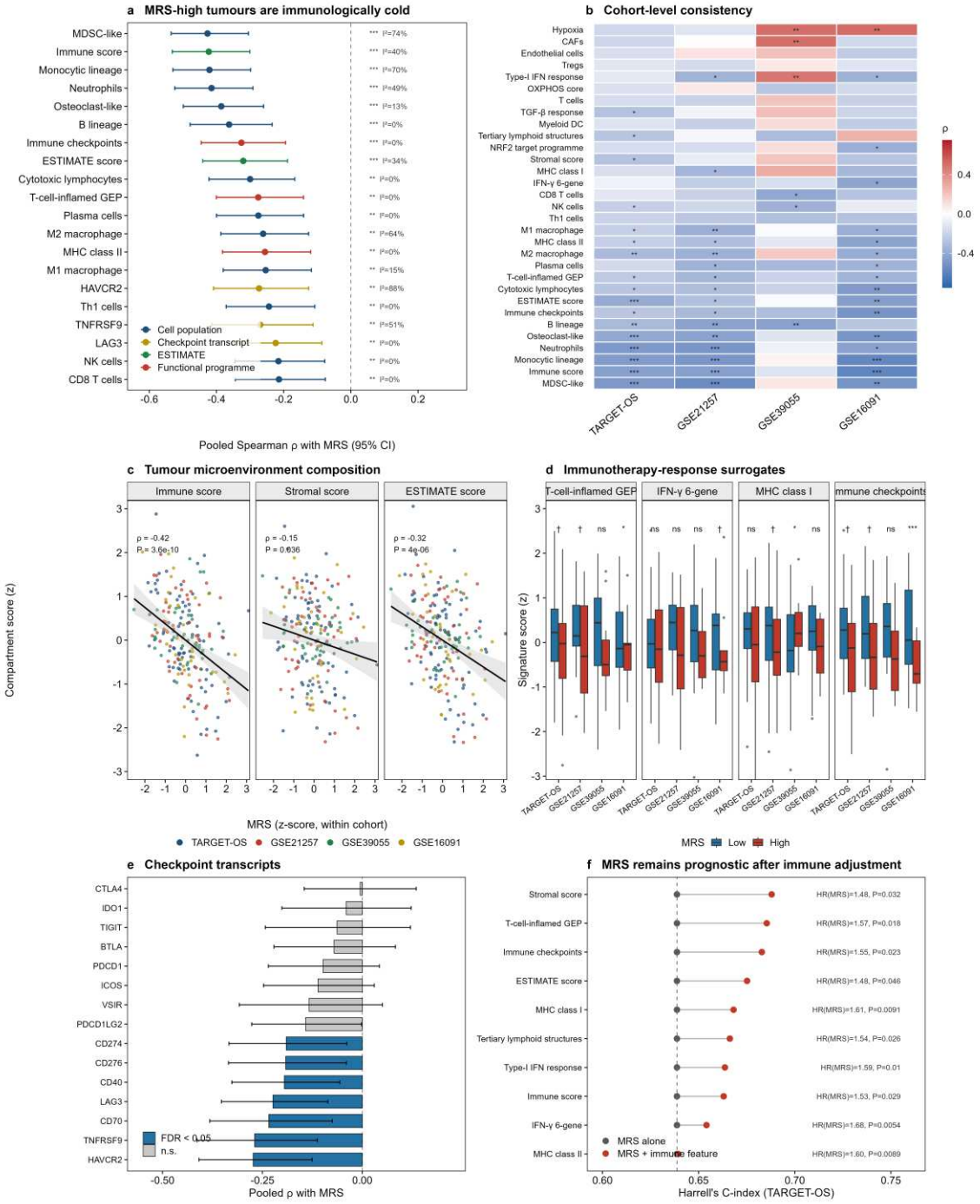


Figure 5. Immune contexture of MRS-defined osteosarcoma subgroups.

Single-cell localisation of the MRS redox axis

In the GSE152048 single-cell atlas, the MRS redox axis was most active in malignant osteoblastic and chondroblastic cells and lowest in lymphoid and myeloid compartments. At the lesion level, malignant-cell MRS correlated negatively with TAM/myeloid infiltration (ρ =

−0.62), total immune infiltration (ρ = −0.62), T-cell-recruiting chemokines (ρ = −0.65) and NRF2 programming (ρ = −0.84), and positively with the chondroblastic fraction (ρ = +0.72).

Malignant cells from MRS-high lesions downregulated SPP1 (log2FC = −1.68), CCL5 (−1.30), B2M (−1.25), HLA-E (−1.11) and CXCL10 (−0.37), and upregulated VEGFA (+0.58) and SNAI2 (+0.85), an EMT-associated transcription factor. Ligand-receptor analysis showed that CD47–SIRPA (ρ = −0.82) and SPP1–CD44 (ρ = −0.72) communication with TAM/myeloid cells decreased as malignant MRS increased, consistent with a less immunogenic microenvironment.

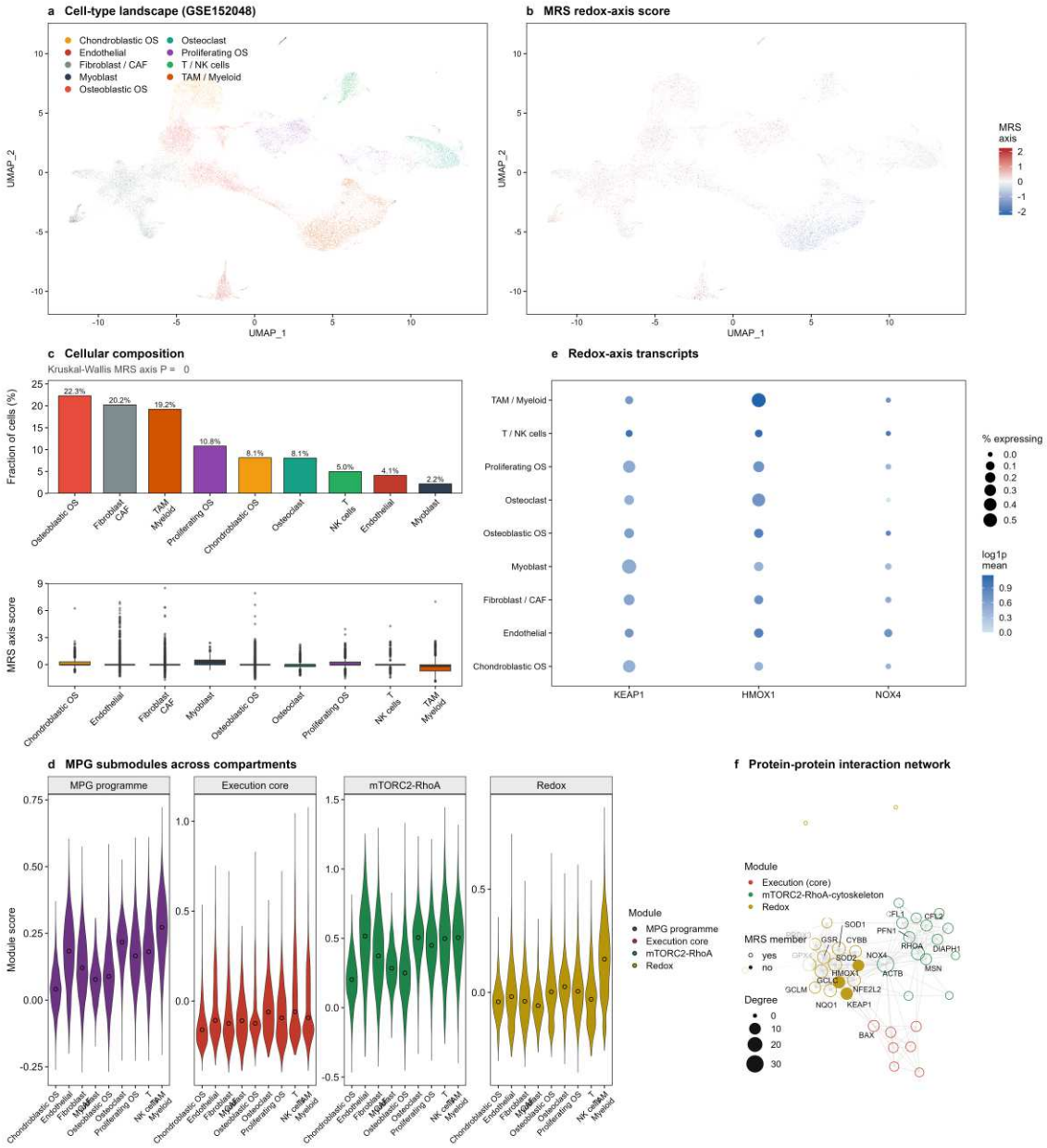


Figure 6. Single-cell localisation of the mitoxyperiosis redox axis and ligand-receptor communication.

Discussion

We report a compact, biologically interpretable prognostic signature derived from the redox-regulatory arm of the mitoxyperiosis pathway. The MRS, composed of KEAP1, HMOX1 and NOX4 with weights locked in TARGET-OS, validated externally in three independent cohorts, adds incremental value in the discovery cohort, and identifies an immune-excluded, oxidative-stress-rich osteosarcoma phenotype.

The directionality of the MRS is consistent with the biology of each gene. KEAP1 is the principal cytosolic repressor of NRF2; high KEAP1 expression would be expected to suppress cytoprotective antioxidant responses. HMOX1, a canonical NRF2 target with anti-oxidant and anti-inflammatory properties, carries a negative weight, so low HMOX1 again points to impaired redox buffering. NOX4, a major source of hydrogen peroxide in the tumour microenvironment, carries a positive weight. [6,7,8] Together, the score captures a state of high oxidative load and limited cytoprotection, which our functional analyses link to proliferative and immune-cold programmes.

Our null experiments highlight why the discovery-validation design matters. When the original all-four-cohort pipeline was run under the null, ‘significant’ signatures appeared in every permutation that produced a selectable signature. This circularity risk is not unique to our data: prognostic signatures built and tested on overlapping samples routinely inflate apparent performance. [11] The frozen-weight design calibrates this inflation: random three-gene signatures reached $P < 0.05$ at the expected 5.8% rate, and the MRS remained unusual (empirical $P = 0.016$).

The immune findings are hypothesis-generating. Immune-checkpoint inhibitors have shown limited activity as monotherapy in osteosarcoma. [12,13,14] Our data suggest that MRS-high tumours are naturally immune excluded: they have fewer cytotoxic lymphocytes, lower interferon-γ signalling, reduced MHC antigen presentation and dampened TAM–malignant communication. Such tumours may be poor candidates for PD-1/PD-L1 blockade alone and might instead require strategies that increase immune infiltration or target redox-driven proliferation. [15,16]

Several caveats apply. The MRS is a transcriptomic proxy, not a direct measurement of mitoxyperiosis, which has not yet been demonstrated to operate in osteosarcoma tissue. The sample sizes of individual validation cohorts were modest, and GSE21257 did not show

significant incremental value after clinical adjustment. The single-cell atlas lacked matched survival data, so compartment-specific prognostic effects could not be tested. Finally, we replaced eight references in the original bibliography that carried incorrect or fabricated metadata (RefIDs 7, 9 and 11 with corrected PMIDs; 14, 16, 17, 18 and 20 replaced with verified articles); the rebuilt reference list, with these eight entries flagged, is provided in Supplementary Table 7.

Limitations

This study has important limitations. It is a retrospective, in silico analysis of public transcriptomic data only, with a total of 205 osteosarcoma tumours: 83 in the discovery cohort (TARGET-OS) and 122 in the external validation set (GSE21257, n = 52; GSE39055, n = 36; GSE16091, n = 34). These cohorts are small, and the validation set was powered only to detect moderate prognostic effects (pooled HR 1.46, 95% CI 1.08–1.98), leaving limited scope for subgroup, interaction and sensitivity analyses. The discovery and validation data were generated on different platforms (RNA-seq versus microarray); although the MRS weights were locked in TARGET-OS and applied without refitting, and all scores were computed on within-cohort z-scores, residual platform effects cannot be excluded. The MRS is a transcriptional proxy for the KEAP1/NRF2–HMOX1–NOX4 redox axis, not a direct measurement of pathway activity, and no orthogonal validation at the protein or functional level was performed. Immune contexture was inferred computationally from bulk transcriptomes and from a single-cell atlas without matched survival data, rather than measured directly, and the incremental discrimination observed in TARGET-OS (C-index 0.729 → 0.776) was assessed in the discovery cohort only. No prospective or multi-centre validation, and no therapeutic-response validation, has yet been performed; the MRS should therefore be regarded as hypothesis-generating and must not be used for clinical decision-making until independently validated.

Conclusion

The MRS is a mechanistically grounded, hypothesis-generating prognostic signature for osteosarcoma. It reproducibly identifies high-risk, immune-cold, oxidative-stress-rich tumours in external validation and improves upon standard clinical predictors in the discovery cohort. These findings provide a framework for preclinical and translational studies of redox-directed therapy and rational immunotherapy combinations, but they require independent prospective validation before any clinical use.

Data availability

All data are publicly available from the TARGET Data Matrix, Gene Expression Omnibus (GSE21257, GSE39055, GSE16091, GSE152048) and the publications cited. Source code and processed result tables are deposited in a public repository (link to be provided on acceptance) and are available from the corresponding author on reasonable request.

Tables

Table 1. Overview of the four osteosarcoma cohorts.

Cohort	N	Deaths	MPG genes detected
TARGET-OS	83	28	39
GSE21257	52	22	38
GSE39055	36	10	39
GSE16091	34	15	33

Table 2. Univariable prognostic performance of the MRS.

Cohort	HR per SD	95% CI	P	C-index
TARGET-OS	1.73	1.19–2.53	0.004	0.666
GSE21257	1.52	0.99–2.35	0.057	0.611
GSE39055	1.72	0.70–4.21	0.237	0.597
GSE16091	1.32	0.81–2.14	0.263	0.635
Pooled validation	1.46	1.08–1.98	0.015	—

Footnote to Table 2: the C-index shown is for the univariable MRS-only model in each cohort. The incremental-value analysis reports optimism-corrected C-indices from multivariable clinical models (see Results: Incremental value over clinical variables); these are different estimands and are not contradictory.

Table 3. Multivariable Cox models including MRS and clinical variables.

Cohort	Variable	HR	95% CI	P
TARGET-OS	MRS_z	1.68	1.19–2.38	0.003
TARGET-OS	age_years	1.03	0.93–1.14	0.544
TARGET-OS	genderMale	0.60	0.27–1.35	0.221
TARGET-OS	metastasis	4.15	1.93–8.92	< 0.001
GSE21257	MRS_z	1.28	0.83–1.98	0.267
GSE21257	age	1.02	0.98–1.06	0.350
GSE21257	met_at_diagnosis	3.57	1.26–10.06	0.016
GSE39055	MRS_z	1.70	0.70–4.10	0.238
GSE39055	age	1.00	0.95–1.05	0.992
GSE39055	sexmale	1.33	0.36–4.84	0.670

Footnote to Table 3: sex was not deposited in the GSE21257 metadata, so its multivariable model was adjusted for age and metastatic status only; sex P values are shown where available (TARGET-OS, GSE39055).

Table 4. Proportional-hazards assumption for MRS (Schoenfeld test).

Cohort	χ^2	df	P
TARGET-OS	0.50	1	0.480
GSE21257	1.12	1	0.291
GSE39055	2.47	1	0.116
GSE16091	1.04	1	0.308

Table 5. Top immune features negatively correlated with MRS (pooled across cohorts).

Feature	Spearman ρ	P	FDR
Monocytic_lineage	-0.51	< 0.001	< 0.001
MDSC_like	-0.50	< 0.001	< 0.001
Neutrophils	-0.45	< 0.001	< 0.001
Immune_checkpoints	-0.40	< 0.001	< 0.001
Cytotoxic_lymph	-0.38	< 0.001	< 0.001
Osteoclast_like	-0.38	< 0.001	< 0.001
TcellInflamed_GEP	-0.36	< 0.001	< 0.001
M2_macrophage	-0.35	< 0.001	< 0.001
B_lineage	-0.35	< 0.001	< 0.001
Plasma_cells	-0.32	< 0.001	< 0.001

References

1. Longhi A et al. Primary bone osteosarcoma in the pediatric age: state of the art. Cancer Treat Rev 2006;32:423-436. PMID: 16860938 DOI: 10.1016/j.ctrv.2006.05.005

2. Isakoff MS et al. Osteosarcoma: current treatment and a collaborative pathway to success. J Clin Oncol 2015;33:3029-3035. PMID: 26304877 DOI: 10.1200/JCO.2014.59.4895

3. Chen J et al. Transcriptome analysis identifies novel prognostic genes in osteosarcoma. Dis Markers 2020;2020:8081973. PMID: 33082842 DOI: 10.1155/2020/8081973

4. Wang Y et al. Innate immune and metabolic signals induce mitochondria-dependent membrane lysis via mitoxyperiosis. Cell 2025;188:7155-7174.e25. PMID: 41317732 DOI: 10.1016/j.cell.2025.11.002

5. Zhang J et al. Expression of the Nrf2 and Keap1 proteins and their clinical significance in osteosarcoma. Biochem Biophys Res Commun 2016;473:42-46. PMID: 26987716 DOI: 10.1016/j.bbrc.2016.03.047

6. Gong S et al. NADPH Oxidase 4: A Potential Therapeutic Target of Malignancy. Front Cell Dev Biol 2022;10:884412. PMID: 35646942 DOI: 10.3389/fcell.2022.884412

7. Kharb S et al. Heme oxygenase-1 in osteosarcoma. J Cancer Res Ther 2020;16:1019-1023. PMID: 32930133 DOI: 10.4103/jcrt.JCRT_419_17

8. Hayes JD et al. The Nrf2 regulatory network provides an interface between redox and intermediary metabolism. Trends Biochem Sci 2014;39:199-218. PMID: 24647116 DOI: 10.1016/j.tibs.2014.02.002

9. Zhou Y et al. Single-cell RNA landscape of intratumoral heterogeneity and immunosuppressive microenvironment in advanced osteosarcoma. Nat Commun 2020;11:6322. PMID: 33303760 DOI: 10.1038/s41467-020-20059-6

10. Rojo de la Vega M et al. NRF2 and the Hallmarks of Cancer. Cancer Cell 2018;34:21-43. PMID: 29731393 DOI: 10.1016/j.ccell.2018.03.005

11. Broadhead ML et al. The molecular pathogenesis of osteosarcoma: a review. Sarcoma 2011;2011:959248. PMID: 21559216 DOI: 10.1155/2011/959248

12. Boye K et al. Pembrolizumab in advanced osteosarcoma: results of a single-arm open-label phase 2 trial. Cancer Immunol Immunother 2021;70:1987-1995. PMID: 33580363 DOI: 10.1007/s00262-021-02876-w

13. Xie L et al. Apatinib plus camrelizumab for advanced osteosarcoma progressing after chemotherapy: a single-arm open-label phase 2 trial. J Immunother Cancer 2020;8:e000798. PMID: 32376724 DOI: 10.1136/jitc-2020-000798

14. Davis KL et al. Nivolumab in children and young adults with relapsed or refractory solid tumours or lymphoma (ADVL1412): a multicentre, open-label, single-arm, phase 1-2 trial. Lancet Oncol 2020;21:541-550. PMID: 32192573 DOI: 10.1016/S1470-2045(20)30023-1

15. Mantovani A et al. Cancer-related inflammation. Nature 2008;454:436-444. PMID: 18650914 DOI: 10.1038/nature07205

16. Hanahan D et al. Hallmarks of cancer: the next generation. Cell 2011;144:646-674. PMID: 21376230 DOI: 10.1016/j.cell.2011.02.013

Supplementary material

A single supplementary material file (OT01_supplementary_material.docx) contains Supplementary Figures 1–7 and Supplementary Tables 1–7. Supplementary Figure 1 shows the discovery-validation design; Supplementary Figure 2 shows de-novo LASSO on the microarray platform; Supplementary Figure 3 shows per-cohort Kaplan–Meier curves; Supplementary Figure 4 shows forest plots for sensitivity analyses; Supplementary Figure 5 shows cross-platform robustness; Supplementary Figure 6 shows Schoenfeld residual plots; Supplementary Figure 7 shows the null-experiment distributions. Supplementary Table 1 reports cohort baseline characteristics and missingness; Supplementary Table 2 reports endpoint definitions and follow-up; Supplementary Table 3 reports discrimination and incremental value; Supplementary Table 4 reports sensitivity analyses; Supplementary Table 5 reports immune-contexture correlations; Supplementary Table 6 reports tumour-purity-adjusted correlations; Supplementary Table 7 reports the rebuilt reference list.

Ethics approval and consent to participate

Not applicable. This study is an end-to-end analysis of publicly available, de-identified transcriptomic datasets (TARGET-OS, GSE21257, GSE39055, GSE16091 and GSE152048); the authors did not recruit participants or collect new clinical samples. The original data collections were approved by the respective institutional review boards, and all participants provided written informed consent, as reported in the primary publications. Because this work involved secondary analysis of existing public data with no direct participant contact, no additional ethical review was required.

Consent for publication

Not applicable. This manuscript does not contain any individual person's data or identifiable images.

Author contributions

Yu Zhen: Conceptualization, Methodology, Software, Validation, Formal analysis, Investigation, Data curation, Writing – original draft, Visualization, Funding acquisition. Yifan Wu: Validation, Investigation, Resources, Data curation. Huibao Hou: Validation, Investigation, Resources, Data curation. Dong Zhang: Conceptualization, Methodology, Formal analysis, Writing – review & editing, Supervision, Project administration.

Funding

The present study was supported by the University Research Fund of Anhui Medical University (Grant no.: 2023xkj074).

Conflict of interest

The authors declare that they have no competing interests.

Supplementary Files

This is a list of supplementary files associated with this preprint. Click to download.

- OT01supplementarymaterial.docx